Materials Physics and Mechanics 47 (2021) 885-895
Research article

Received: July 30, 2020
Accepted: November 16, 2021

MATHEMATICAL MODELLING OF ICE BEAM DEFLECTION DYNAMICS

A.M. Reztsova✉

Peter the Great St. Petersburg Polytechnic University, 29 Politechnicheskaya St., St. Petersburg, 195251, Russia

✉ angelina-rezcova@mail.ru

Abstract. The assessment of stresses arising from the interaction of the ice field and inclined structures is an important part of research in ice mechanics. For these purposes, various mathematical tools are used, including mechanical models of beams. The article presents solutions for the equation of dynamic deflection of a beam with different boundary conditions, as well as taking into account the influence of a liquid located under the ice field. The inclusion of the base reaction in the beam deflection equation allows us to obtain an alternative model, which in some cases turns out to be more accurate than others. The obtained solutions are tested on the results of our own experiments conducted in an ice basin with model ice. In the experiments, the velocity of structures was varied; force projections, time, and place of the ice beam failure were recorded.

Keywords: cantilever beam, bending dynamics, ice-structure interaction, model ice

Acknowledgements*. This work is made as a part of the project 0784-2020-0021 supported by the Ministry of Science and Higher Education of the Russian Federation.*

Citation: Reztsova A.M. Mathematical modelling of ice beam deflection dynamics // Materials Physics and Mechanics. 2021, V. 47. N. 6. P. 885-895. DOI: 10.18149/MPM.4762021_8.

1. Introduction

A significant part of the research on the impact of ice on marine structures is devoted to the interaction of the ice field with an inclined plane. In the Arctic conditions, ice fields pose danger to offshore structures. Variation of the inclination angle governs a reduction in the load on these structures.

Failure of ice when interacting with an inclined plane is a complex process consisting of several stages. This paper considers a stage lasting until the first break appears in the ice sheet. The main type of inclined ice plane failure is bending; stresses arising due to compression of the material also have a slight impact [1,2]. For the purpose of a detailed study of the above-mentioned processes, model tests on the destruction of ice by an inclined structure have been conducted; the experiments have determined the components of the force load on the model of the inclined structure.

In recent decades, the issue of the interaction of ice with an inclined plane has been actively studied by well-known scientists in the field of ice mechanics, such as Frederking R. [3,4], Croasdale K. [5], Kheisin D. [6,7], Dempsy J. [8] and Maattanen U. [9]. Frederking investigated the behavior of the ice cover acting on an inclined structure at its destruction, the

http://dx.doi.org/10.18149/MPM.4762021_8

types of occurring cracks, and the stages of their formation. Paper [4] presents the graphs on the dependence of the maximum value of the horizontal load on the inclined plane on the friction coefficient, ice thickness, etc. Kheisin was the first to describe the linear theory of the dynamic phenomena occurring in the ice sheet. For example, he considered the deformation of an ice field as bending of a plate under the action of a concentrated force, taking into account the influence of waves in water using the wave equation or the liquid potential. The main equation considered in [7] in the case of the above-mentioned process is given as $D\nabla^4 w + \rho_1 h\frac{\partial^2 w}{\partial t^2} + \rho_2 g w + \rho_2\frac{\partial \Phi}{\partial t} = P_0 e^{i\omega t}\delta(x,y)$, where the potential of liquid – is $\Phi(x,y,z,t)$, the deflection of the plate – is $w(x,y,t)$, liquid and ice properties are given by the densities $\rho_{1,2}$. The analytical integration of this equation becomes problematic with the presence of inhomogeneous boundary conditions; thus it requires numerical solutions or simplifications of the geometry [10].

If this equation is simplified, the summand with the liquid potential can be omitted, then the influence of water will be taken into account by the summand with a modulus of a subgrade reaction ($\rho_2 g$), or will be replaced by a coefficient of an added mass. The numerical solution of a two-dimensional problem using the bed coefficient is presented in [11], in [12] the ice field failure is modeled by FDM using the coefficient of an added mass.

This paper presents a comprehensive study of the analytical solution of two equations of the ice field dynamic bending in a one-dimensional case, i.e., the geometry of the ice field is simplified to the case of an ice beam. It is possible to assume that the deflections of the longitudinal sections of the ice field plate slightly differ from each other and coincide with the deflection of the section in the middle line of a plate. Additionally, it is assumed that Young's modulus is constant.

Nomenclature

E – Young's module, Pa;
I – moment of inertia, m^4;
k – coefficient of an elastic foundation (bed), kN/m^3;
ρ – material density, kg/m^3;
h – beam thickness, m;
b – beam width, m;
L – beam length, m.

2. Mathematical model

Modelling the processes of interaction of the ice field with various objects involves simplifying its geometry. The case when the ice field hits an inclined plane is often considered in mechanics as a problem of a beam bending under certain boundary conditions. Accounting for the influence of water, which is under the ice field, requires adding an elastic foundation to the equation and sometimes an added mass. The paper considers both of the cases. The equation of the dynamic deflection of a beam on an elastic foundation is given as [13]

$$\rho h\frac{\partial^2 w}{\partial t^2} + EI\frac{\partial^4 w}{\partial x^4} + kw = 0, \quad (1)$$

where $w(x,t)$ is the desired transverse displacement $I = \frac{bh^3}{12}$ – is the moment of inertia for a rectangular beam, ρ is the density of ice.

It is necessary to set four boundary conditions for equation (1). When the end of the beam, which represents the free edge of an ice field, hits an inclined structure at speed v, it instantly receives a vertical component of the speed, depending on the inclination angle (Figure 1 (a)). It is assumed that the forces are applied to the neutral axis of the beam, then the

condition of zero bending moment is set at the free end. The boundary conditions will be as follows:

$$w(0,t) = v\ t\ ctg\varphi;\ \frac{\partial^2 w}{\partial x^2}(0,t) = 0;\ w(\infty,t) = 0;\ \frac{\partial w}{\partial x}(\infty,t) = 0. \quad (2)$$

This paper also considers another possible approach to set boundary conditions for this type of problem, which is force boundary conditions. When the ice edge comes into contact with an inclined plane, brittle failure occurs due to the fragility of the material. At the free end, a contact surface is formed which gives as a lever arm to the moment of the longitudinal component $\boldsymbol{P_x}$ of the force **N** (Fig. 1(b)). The bending moment for a rectangular beam, taking into account the sign is given as $M = -\frac{h|\boldsymbol{P_x}|}{2}$. The transverse component of the force $\boldsymbol{F_z}$ initiates the setting of the boundary condition for setting the external force at the end $F = |\boldsymbol{F_z}|$.

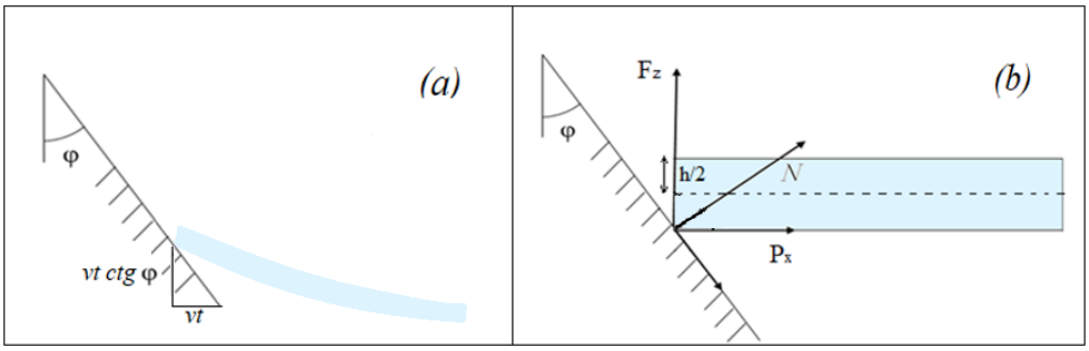

Fig. 1. Simplified models for two types of boundary conditions of the problem of the bending ice beam failure due to interaction with an inclined structure: (a) – the first type of boundary conditions; (b) – the second type of boundary conditions

A model experiment in an ice tank allows us to obtain force measurements P_x, F_z using dynamometers. Figure 2 shows an example of measuring the transverse component P_x during 1 minute in the experiment on the destruction of a simulated ice beam by an inclined plane. The linear section of the load growth characterizes the movement of the ice field along with the plate until the crack is formed.

The time dependence according to the linear law can be expressed in terms of the proportionality coefficients, which are obtained from the linear approximation of discrete signals from the sensor. Then $P_x = k_x t,\ F_z = k_z t$ (Fig. 3).

Thus, the force and moment included in the boundary conditions will be written as follows: $F = F(t) = C_F \cdot t, M = M(t) = C_M \cdot t$, where $C_F = k_z, C_M = k_x \frac{h}{2}$. As a result, we obtain:

$$EI\ \frac{\partial^2 w}{\partial x^2}(0,t) = -C_M t;\ EI\frac{\partial^3 w}{\partial x^3}(0,t) = C_F t;\ w(\infty,t) = 0;\ \frac{\partial w}{\partial x}(\infty,t) = 0, \quad (3)$$

The initial conditions are zero:

$$w(x,0) = 0;\ \frac{\partial w}{\partial t}(x,0) = 0. \quad (4)$$

The analytical solution of the partial differential equation (1) under zero initial conditions and boundary conditions (2) or (3) can be obtained using the Laplace integral transforms:

$$W(x,p) = \int_0^{+\infty} w(x,t)e^{-pt}dt,$$

where $p = \alpha + i\omega$ is a complex parameter. The transition to a new parameter allows to omit the time variable; thus, a new differential equation is obtained, the solution of which is expressed in terms of elementary functions.

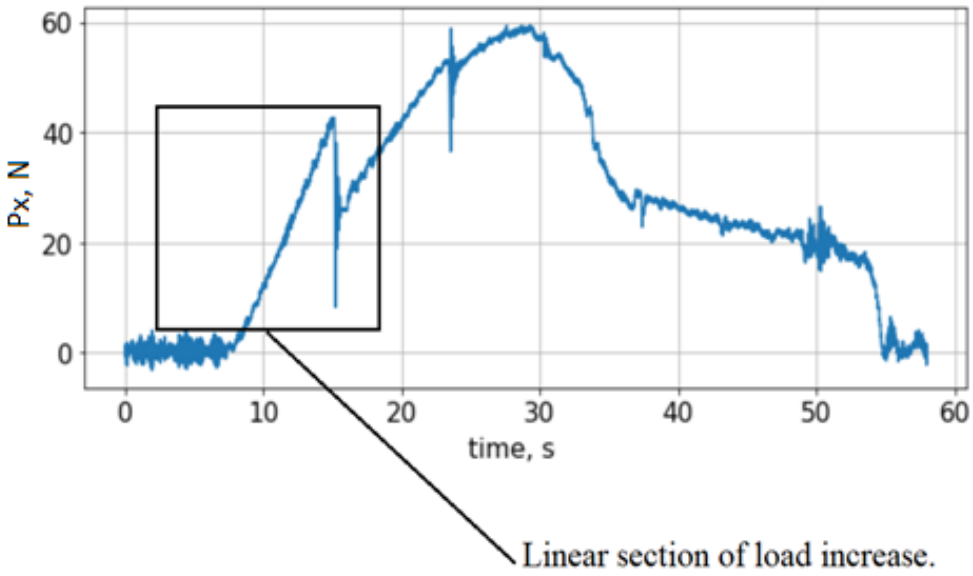

Fig. 2. Graph of loads on the inclined plane recorded during the experiment for the speed of movement $v = 5$ mm/s

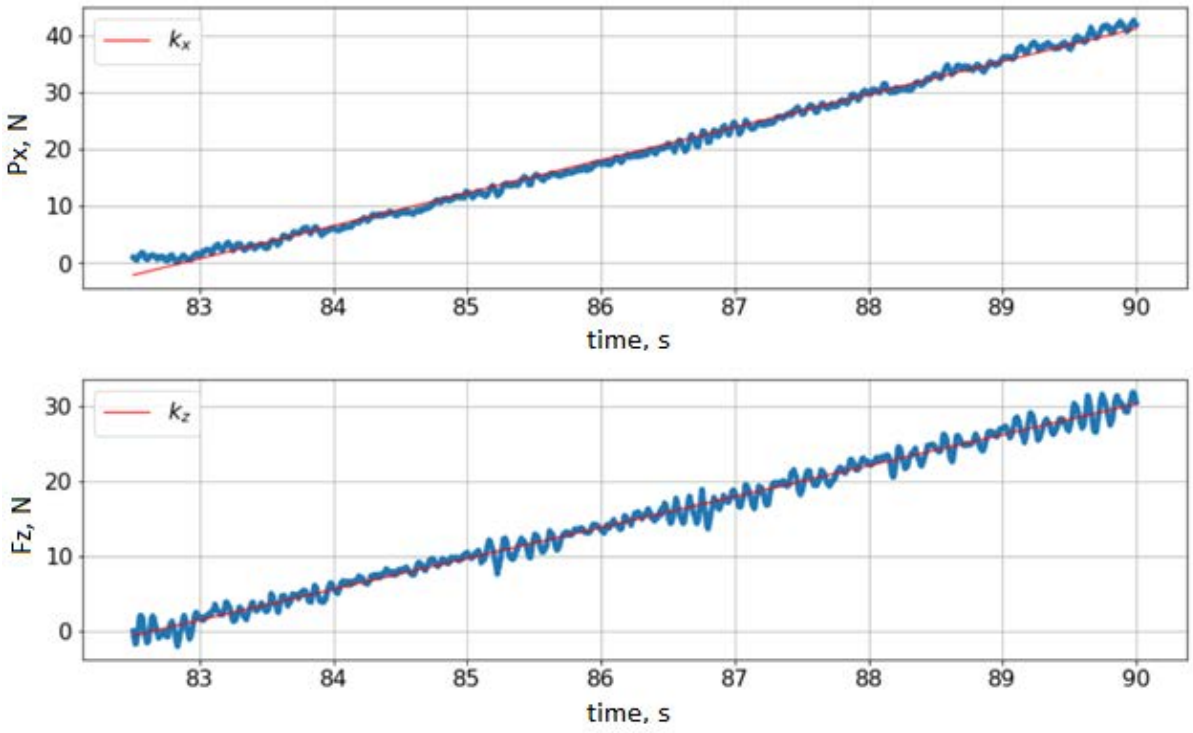

Fig. 3. Graphs of linear load sections for force components P_x and F_z at speed $v = 5$ mm/s. The red line indicates the linear function obtained by approximating grid functions by the least-squares method.

The $w_1(x,t)$ denotes a solution of equation (1) for mixed boundary conditions of type (2), $w_2(x,t)$ – the solution of the equation (1) for force boundary conditions of type (3).

$$w_1(x,t) = \frac{1}{2\pi i}\oint e^{pt}e^{-\beta x}\frac{v}{p^2}\cos\beta x\, dp, \quad (5)$$

$$w_2(x,t) = \frac{1}{2\pi i}\oint e^{pt}e^{-\beta x}\left[\frac{C_M\beta + C_F}{2p^2\beta^3}\cos\beta x - \frac{C_M}{2p^2\beta^2}\sin\beta x\right] dp, \quad (6)$$

where $= \frac{\sqrt[4]{\frac{p^2+\kappa}{\gamma}}}{\sqrt{2}}, \frac{EI}{\rho h} = \gamma, \frac{k}{\rho h} = \kappa.$

To go to the original coordinates, it is necessary to carry out the inverse transformation, calculate the Riemann-Mellin integral. At this stage, difficulties may arise mainly related to the choice of the integration contour, bypassing the branching points, and deducting the residue of the function of a complex variable. Let us bring the solution to the final version for two boundary conditions:

$$w_1(x,t) = vt\ ctg\varphi\ e^{-\frac{\sqrt{2}}{2}\sqrt[4]{\frac{k}{EI}}x}\ cos(\frac{\sqrt{2}}{2}\sqrt[4]{\frac{k}{EI}}x), \tag{7}$$

$$w_2(x,t) = \frac{te^{-\frac{\sqrt{2}}{2}\sqrt[4]{\frac{k}{EI}}x}}{\sqrt{\frac{k}{EI}}}\left[(C_M + \frac{\sqrt{2}C_F}{\sqrt[4]{\frac{k}{EI}}})\ cos(\frac{\sqrt{2}}{2}\sqrt[4]{\frac{k}{EI}}x) - C_M sin(\frac{\sqrt{2}}{2}\sqrt[4]{\frac{k}{EI}}x)\right]. \tag{8}$$

In this form, the solutions show only a deflection. To study the process of the ice field failure, the stresses arising in the material are of greater interest. Let us assume that the condition for initiating destruction is achieving the ultimate bending strength of the beam material $\max_{0\le x\le\infty, 0\le t\le\infty}\ \sigma(x,t) > \sigma_s$. Knowing the analytical deflection formulas expressed in this paper by formulas (7) and (8), we can obtain the stresses. For two models, we will obtain the following expressions for the stresses:

$$\sigma_1(x,t) = 2E\frac{h}{2}vt\ ctg\varphi\sqrt[4]{\frac{k}{EI}}e^{-\frac{\sqrt{2}}{2}\sqrt[4]{\frac{k}{EI}}x}\ cos(\frac{\sqrt{2}}{2}\sqrt[4]{\frac{k}{EI}}x), \tag{9}$$

$$\sigma_2(x,t) = E\frac{h}{2}te^{-\frac{\sqrt{2}}{2}\sqrt[4]{\frac{k}{EI}}x}\left[(C_M + \frac{\sqrt{2}C_F}{\sqrt[4]{\frac{k}{EI}}})\ sin(\frac{\sqrt{2}}{2}\sqrt[4]{\frac{k}{EI}}x) + C_M cos(\frac{\sqrt{2}}{2}\sqrt[4]{\frac{k}{EI}}x)\right]. \tag{10}$$

Formulas (7)-(10) presented in this chapter will be used to model the behavior of the ice field in the conditions of the model experiments on the destruction of ice when coming into contact with an inclined plane.

3. Taking into account the additional masses in the problem with a beam movement

When a body moves in an inviscid liquid, its inertial properties are determined by the added masses. For bodies of various shapes moving in a homogeneous liquid, these characteristics are well studied and presented in numerous papers, for example, [14].

The formulas for the added mass of a rectangle are given in [15,16]. The coefficient of added masses is equal to $k_{11} = \frac{\lambda_{11}}{\rho bd}$. For a beam with the parameters $\frac{d}{b} = 10$ the $k_{11} \approx 2.2$.

Similarly (1), we can write the equation of the beam deflection, where the influence of the hydraulic foundation is taken into account by adding the added mass

$$(1 + k_{11})\rho h\frac{\partial^2 w}{\partial t^2} + EI\frac{\partial^4 w}{\partial x^4} = 0. \tag{11}$$

The boundary conditions are set as follows:

$$w(0,t) = vt;\ \frac{\partial^2 w}{\partial x^2}(0,t) = 0;\ w(\infty,t) = 0;\ \frac{\partial w}{\partial x}(\infty,t) = 0, \tag{12}$$

where v is the speed of movement of a structure. The initial conditions are zero:

$w(x,0) = 0;\ \frac{\partial w}{\partial t}(x,0) = 0.$

In this formulation, the problem has been solved by Osipenko N.M. [17], and the following solution has been obtained:

$$w_3(x,t) = -\frac{t}{2}\int_\eta^\infty \frac{S(\eta)}{\eta^{\frac{1}{2}}}d\eta + \frac{t}{2}\int_\eta^\infty \frac{S'^{(\eta)}}{\eta^{\frac{3}{2}}}d\eta, \eta = \frac{1}{4a^2}\left(\frac{x^2}{t}\right), a = \left(\frac{EI}{c\rho h}\right)^{\frac{1}{4}},$$

$$S(\eta) = \frac{2^{3/2}}{\pi} v cos\eta. \quad (13)$$

$$w_3(x,t) = \frac{3vt}{\sqrt{\pi}}\left[2C\left(\sqrt{\frac{2\eta}{\pi}}\right) - 1\right] - \frac{2\sqrt{2}vt}{\pi}\frac{sin\eta}{\sqrt{\eta}}, \quad (14)$$

where $C(x) = \int_0^x \cos(t^2)dt$ is the Fresnel C integral.

The type of the solution (14) is a simplification of the solution (13) obtained in the article [17]. However, when calculating the stresses according to the formula given earlier, the question arises about the continuity of the resulting function σ:

$$\sigma_3(x,t) = E\frac{h}{2}\left[-\frac{12vx}{\pi^3 a^3\sqrt{2t}} sin\left(\frac{x^2}{a^2}\frac{1}{2\pi t}\right) + \frac{\sqrt{2}v}{2a\pi x} cos\left(\frac{x^2}{a^2}\frac{1}{2\pi t}\right) - \frac{2\sqrt{2}vta}{\pi x^3} sin\left(\frac{x^2}{a^2}\frac{1}{2\pi t}\right)\right]. \quad (15)$$

The formula for stresses cannot be used at $x = 0$, since it is discontinuous at this point. It will be convenient to use an approximate form of the solution for small values of the time variable in the form of $w_3(x,t) \approx \frac{12k_z}{Eh^3}\left[\frac{2B^3}{15}t^{5/2} - \frac{B^2}{4}xt^2 + \frac{x^3 t}{6} - \frac{x^5}{2B^2}\right]$, where $B \approx 1.04(\frac{h\sqrt{E/\rho}}{\sqrt{c}})^{1/2}$. Since $k_z = const$, the stresses are approximately expressed as $\sigma_3(x,t) \approx \frac{6k_z}{h^2}x\left[t - 10\frac{x^2}{B^2}\right]$.

These approximated formulas work well for small durations; with the growth of t, the solution shows a large deviation from the empirical data.

4. Experimental Results

To verify the results, the model tests on the interaction of the ice field with an inclined plane have been carried out in the ice basin of the Krylov State Research Centre (St. Petersburg, Russia). The simulated ice for these tests is made according to the Fine Grain technology. The temperature of ice freezing was -25°C. The thickness of the frozen ice averaged h=50 mm along the entire length of the ice tank. Rectangular beams are cut out of a homogeneous field with a width of b = 0.5 m and a length of L = 1.5 m. The beam width was chosen according to the width of the existing model with an inclined wall. The length was chosen as long as possible, due to considerations of the technical feasibility of manufacturing at a given thickness of the ice.

The physical and mechanical properties of the model ice, such as Young's modulus, compressive, and bending strengths, have been measured according to the ITTC standards [18]. Table 1 presents the measured values.

Table 1. Properties of the model ice

Characteristics	Value from the experiment (average)
Density, kg/m3	900
Young's modulus, MPa	24.2
Compressive strength, kPa	28.88
Flexural strength, kPa	22.8

The experiment has used the principle of inverse motion – the ice field is stationary, the inclined plane is fixed on the trolley, and moves along the ice tank. The experimental data have been obtained for velocities (0.0025, 0.005, 0.025) m/s. The failure of the ice beams has been recorded using photo and video equipment. Figure 4 shows the moments of the ice field fracture.

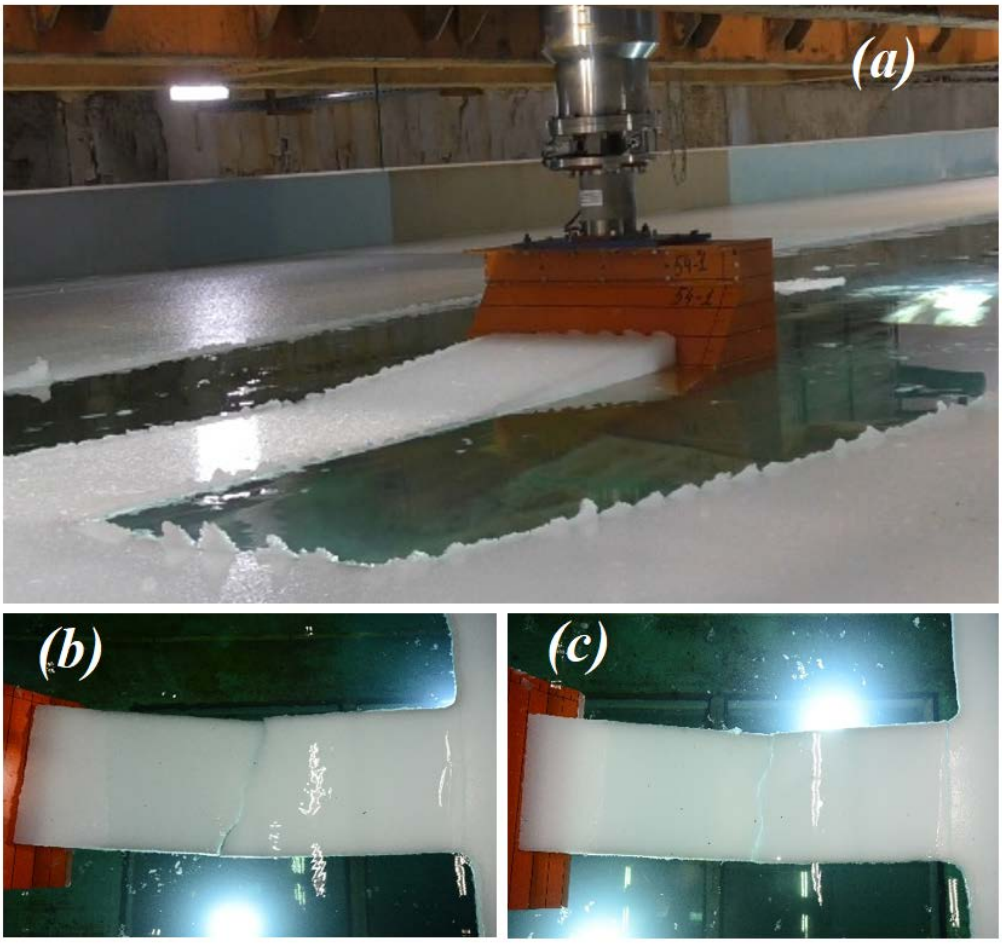

Fig. 4. Images of the experimental installations in the experiment on the interaction of the ice field with the inclined plane at different velocities: (a) 25 mm/s, (b) 5 mm/s, (c) 2.5 mm/s. The angle of inclination is 53°, the thickness of the simulated ice is 0.05 m

The expressions $w_1(x,t), w_2(x,t), w_3(x,t)$ are used to visualize the deflection of the ice field. Figure 5 shows the graphs of the beam deflection in different problem statements and at different time points.

The deflection function for the third equation $w_3(x,t)$ on the considered interval $x \in [0, 1.5]$ m is quite close to the linear function, with only the inclination angle changing in time. The analytical expression obtained for stresses $\sigma_3(x,t)$ in the framework of the model, taking into account the added masses does not fully describe the case of the ice material failure since the maximum value of stress increases significantly with time.

Figure 6 shows the stresses in the ice beam at the time moment of fracture t_{br} for σ_1 and σ_2.

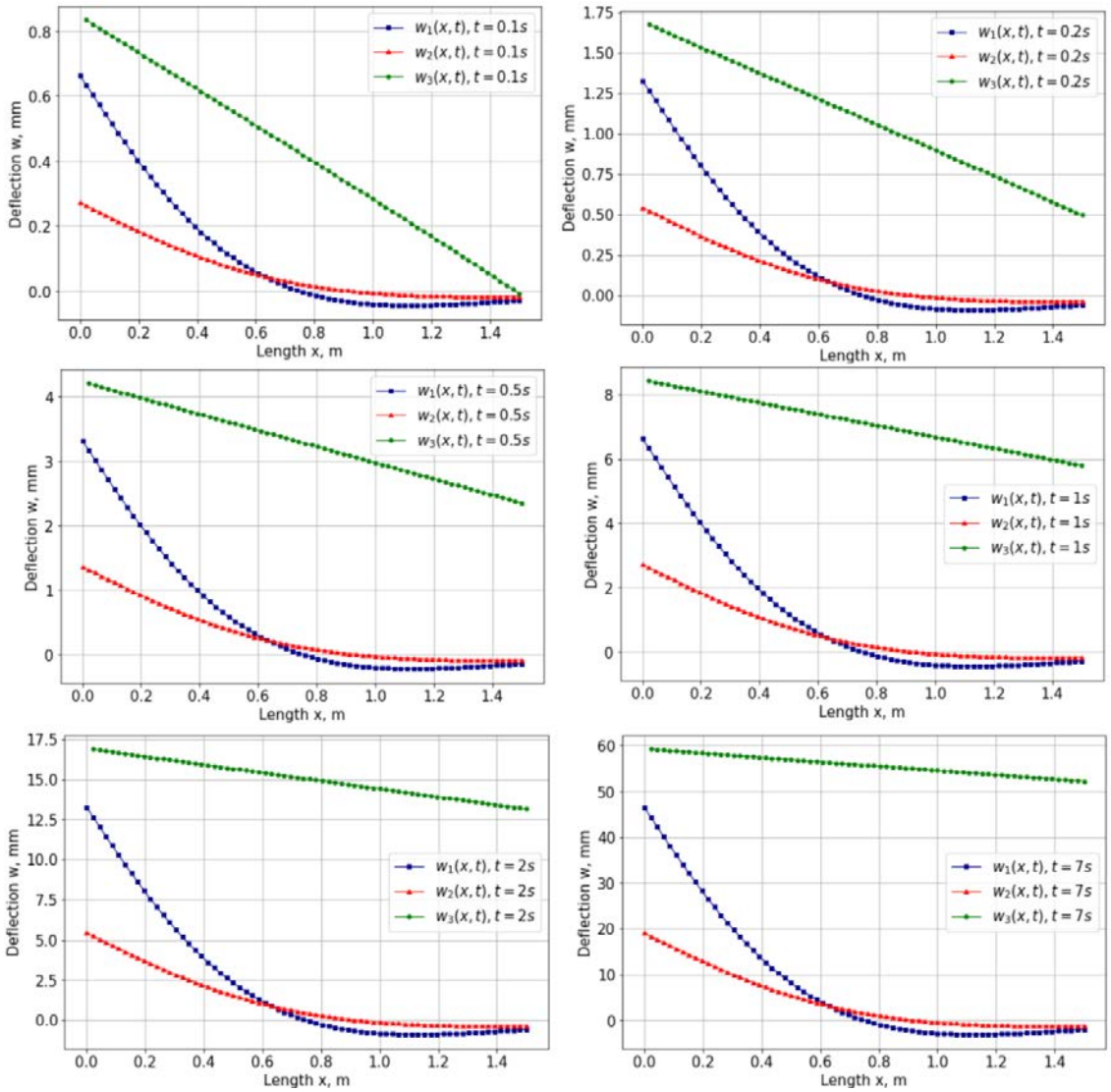

Fig. 5. Deflection plots for three problem statements at different time points for speed $v = 5\ mm/c$. Solid red line – solution $w_1(x,t)$ taking into account the elastic foundation with mixed boundary conditions; dotted blue line – solution $w_2(x,t)$ taking into account the elastic base with force boundary conditions.; dotted green line – solution $w_3(x,t)$ for a model with an added mass factor

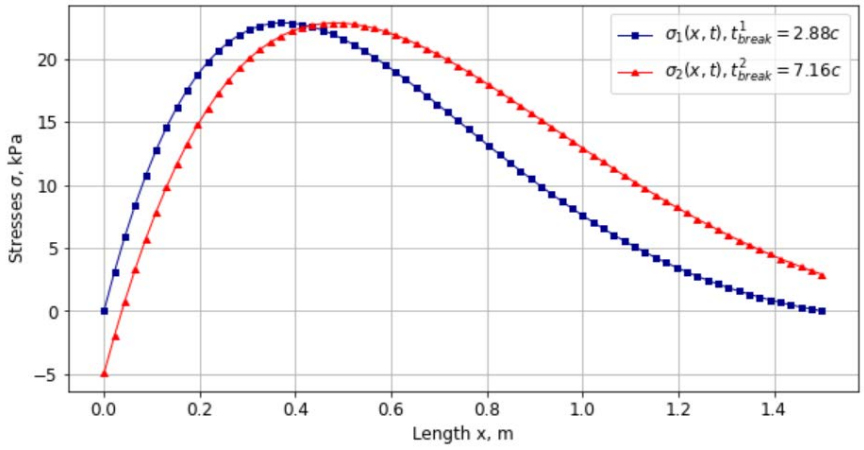

Fig. 6. Stress graphs $\sigma_1(x,t)$ and $\sigma_2(x,t)$, shown at the moment of the fracture t^1_{break} and t^2_{break} for each statement of the problem, respectively

For the second formulation of the problem, the fracture time is significantly longer than for the first one. According to the stress graphs, the time and place of the breaking point is determined from the following condition $\{x_{break}, t_{break}: \sigma(x_{break}, t_{break}) > \sigma_s\}$. Table 2 below presents a comparison of the experimental results and analytical models.

Table 2. Comparison of the results of two models

Value	Experimental	Model 1	Model 2	Error, model 1	Error, model 2
t_{break}, s	7.2	2.88	7.16	**60%**	**0.5%**
x_{break}, m	0.6	0.37	0.51	**38%**	**15%**

4. Discussion and final remarks

The solutions presented in the form of $w_1(x,t) = vte^{-\frac{\sqrt{2}}{2}\sqrt[4]{\frac{kb}{EI}}x}\cos(\frac{\sqrt{2}}{2}\sqrt[4]{\frac{k}{EI}}x)$ and $w_2(x,t) = \frac{te^{-\frac{\sqrt{2}}{2}\sqrt[4]{\frac{kb}{EI}}x}}{\sqrt{\frac{kb}{EI}}}\left[(C_M + \frac{\sqrt{2}C_F}{\sqrt[4]{\frac{kb}{EI}}})\cos(\frac{\sqrt{2}}{2}\sqrt[4]{\frac{k}{EI}}x) - C_M\sin(\frac{\sqrt{2}}{2}\sqrt[4]{\frac{k}{EI}}x)\right]$ contain a time variable raised to the first power. This type of solution is associated with boundary conditions in which the force and moment depend linearly on time. Proper functions of the differential equation are reduced with expressions in the integration constants, which leaves only a linear factor t in the solution. It turns out that $\frac{\partial^2 w}{\partial t^2} \equiv 0$ for any values of the variables x and t. In this case, the statement of the dynamic problem-equation (1) - does not make any sense. In the solution of equation (11) in the form of $w(x,t) = \frac{3vt}{\sqrt{\pi}}\left[2C\left(\sqrt{\frac{2\eta}{\pi}}\right) - 1\right] - \frac{2\sqrt{2}vt}{\pi}\frac{sin\eta}{\sqrt{\eta}}$ the deflection function has a complex dependence on the time variable. Here $\frac{\partial^2 w}{\partial t^2} \neq 0$.

However, the solutions w_1, w_2 with a linear dependence on t describe the experiment quite well in comparison with w_3, where the deviation from the experiment is observed at short durations already. In the second solution, the time of the fracture coincides with the time of the ice beam fracture with an accuracy of 0.5%, which has been recorded on the video.

5. Conclusion

This paper obtains solutions of the equations of dynamic bending of the beam on an elastic foundation and with a coefficient of added masses, which are used to model the fracture process in the ice field interacting with an inclined plane [19]. For each equation, the formulation of boundary conditions corresponding to the physical process and mathematical considerations, namely, the continuity of the deflection function, is proposed.

The experiments in the ice tank on the failure of the beams by the inclined plane have been carried out to verify the mechanical models. During the experiments the values of the forces acting on the model with the inclined plane from the side of the ice beam have been recorded by means of a six-component dynamometer; video recording has been made from different angles.

The accuracy of the models in relation to the obtained experimental data differs. The smallest error is given by the model, the coefficients C_M and C_F in the boundary condition of which are based on the readings of the dynamometer. It is believed that coefficients C_M and C_F can be obtained without additional empirical data on the dynamics of loads. For example, in [20] the expressions for coefficients are given in terms of various ice and liquid properties; but determining some parameters is more time-consuming than fixing loads on an inclined plane. The plans for the further development of this issue include determining methods for

the non-empirical determination of force and moment multipliers in linear boundary conditions.

The results presented in this paper are applied to narrow beams. The microstructure of the ice is not taken into account, as well as small cracks that may form inside the material.

References

[1] Lindholm JE, Makela K, Zheng CB. Structure-Ice Interaction for a Bohai Bay Oil Production Project. In: *Proceedings of 3 International Offshore and Polar Engineering Conference*. 1993. p.538-547.

[2] Saeki H, Ono T, Ozaki A. Experimental Study on Forces on a Cone-Shaped and an Inclined Pile Structures. In: *Proceedings of International Conference on Port and Ocean Engineering under Arctic Conditions*. 1979. p.1081–1095.

[3] Frederking RM. Dynamic ice forces on an Inclined Structures. In: *Physics and Mechanics of Ice. IUTAM Symposium.* 1980. p.104-116.

[4] Frederking R, Timco GW. Quantitative Analysis of Ice Sheet Failure Against an Inclined Plane. *Journal of Energy Resources Technology*. 1985;107(3): 381-387.

[5] Croasdale KR, Cammaert AB. An Improved Method for the Calculation of Ice Loads on Sloping Structures in First Year Ice. In: *Proceedings of 1st RAO Conference*. 1993. p.161-168.

[6] Aleynikov SM, Kheisin DE, Shmeleva LA. Vozdejstvie l'da na gidrotehnicheskie sooruzhenija. In: *Mehanika i fizika l'da.* Moscow: Nauka; 1983. p.5-14. (In-Russian)

[7] Kheisin DE. *Dynamics of the ice cover.* Army Foreign Science and Technology Center Washington DC; 1969.

[8] Dempsy JP, Colin Fox, Palmer AC. Ice-slope interaction: Transition in Failure Mode. In: *Proceedings of the OMAE Conference*. Newfoundland, Canada; 1999. p.1-6.

[9] Maattanen U. Ice Sheet Failure against an Inclined Wall. In: *8th IAHR Ice Symposium*. 1986. p.149-158.

[10] Von Bock und Polach RUF, Franz RU. Numerical analysis of the bending strength of model-scale ice. *Cold Regions Science and Technology*. 2015;118: 91-104.

[11] Simakina A, Zvyagin P, Drepin M. A Model for Ice Heterogeneity Affecting Bending Failure Agains an Inclined Structure. In: *Proceedings of the 40th International Conference on Ocean, Offshore and Arctic Engineering OMAE2021*. 2021.

[12] Bolshev AS, Frolov SA. Mathematical modelling of level ice with continental shelf structures interaction. *IOP Conference Series: Earth and Environmental Science*. 2018;193: 012006.

[13] Timoshenko SP, Voinovsky-Krieger S. *Plates and shells*. Moscow: Nauka; 1966. (In Russian)

[14] Korotkin A. *Prisoedinennye massy sudna: Reference.* Leningrad: Sudostroenie; 1986. (In Russian)

[15] Riman IS, Kreps RL. Prisoedinennye massy tel razlichnoj formy. *Works of TsAGI*. 1947;635: 172-188. (In Russian)

[16] Sedov LI. *Ploskie zadachi gidrodinamiki i ajerodinamiki*. Moscow: Nauka; 1966. (In Russian)

[17] Osipenko NM. Dinamika oblamyvanija kromki plavuchego l'da u pregrady. *Vesti gazovoj nauki*. 2019;9: 54-61. (In Russian)

[18] ITTC Recommended Procedures and Guidelines. *Test Methods for Model Ice Properties*. 2014. Available from: https://www.ittc.info/media/8061/75-02-04-02.pdf

[19] Sodhi DS. Dynamic analysis of failure modes on ice sheets encountering sloping structures. In: *Proc. of 6th Offshore Symp*. Houston; 1987. p.281-284.

[20] Sørensen C. Dynamic bending failure of a semi-infinite ice floe hitting a sloping plane. In: *Proc. of 4th POAC '77*. Newfoundl; 1978. p.580-592.

THE AUTHORS

Reztsova A.M.
e-mail: angelina-rezcova@mail.ru
ORCID: 0000-0002-5941-8765